Jurnal Teknologi, 54 (Sains & Kej.) Keluaran Khas, Jan. 2011: 319–12

IMAGE RECONSTRUCTION ALGORITHMS FOR ULTRASONIC TOMOGRAPHY

MOHD HAFIZ FAZALUL RAHIMAN[1*], RUZAIRI ABDUL RAHIM[2] & HERLINA ABDUL RAHIM[3]

Abstract. This paper presented image reconstruction algorithms for use in ultrasonic tomography. There are three types of reconstruction algorithms namely Linear Back Projection, Hybrid Reconstruction and Hybrid Binary Reconstruction. The algorithms have been evaluated on ultrasonic tomography system based on several known phantoms and real objects. The performance of the algorithms have been analysed and discussed at the end of the paper.

Keywords: Reconstruction algorithm; ultrasonic tomography; image processing

Abstrak. Kertas ini membincangkan algoritma pembangunan imej bagi kegunaan dalam tomografi ultrasonik. Terdapat tiga jenis algoritma pembangunan iaitu Linear Back Projection, Hybrid Reconstruction dan Hybrid Binary Reconstruction. Algoritma tersebut telah diuji ke atas sistem tomografi ultrasonik berdasarkan kepada beberapa bayang yang telah dikenalpasti dan objek –objek sebenar. Prestasi algoritma tersebut telah di analisa dan bincangkan pada bahagian akhir kertas ini

Kata kunci: Algoritma pembangunan; tomografi ultrasonic; pemprosesan image; mabuk

1.0 INTRODUCTION

Most of the work in process tomography has focused on the back projection technique. It is originally developed for the X-ray tomography and it also has the advantages of low computation cost [1]. The measurements obtained at each projected data are the attenuated sensor values due to object space in the image plane. These sensor values are then back projected by multiplying with the corresponding normalized sensitivity maps [2]. The back projected data values are

[1-4] Tomography Imaging Research Group, School of Mechatronic Engineering, Universiti Malaysia Perlis, 02600, Arau, Perlis, Malaysia

[2&3] Process Tomography Research Group, Faculty of Electrical Engineering, Universiti Teknologi Malaysia, 81310 UTM Johor Bahru, Johor Darul Ta'azim, Malaysia

* Corresponding author: hafiz@unimap.edu.my

smeared back across the unknown density function (image) and overlapped to each other to increase the projection data density. The process of back projection is shown in Figure 1 and Figure 2.

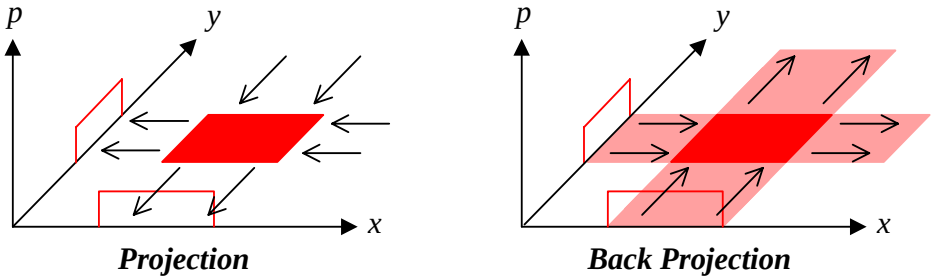

Figure 1 The back-projection method

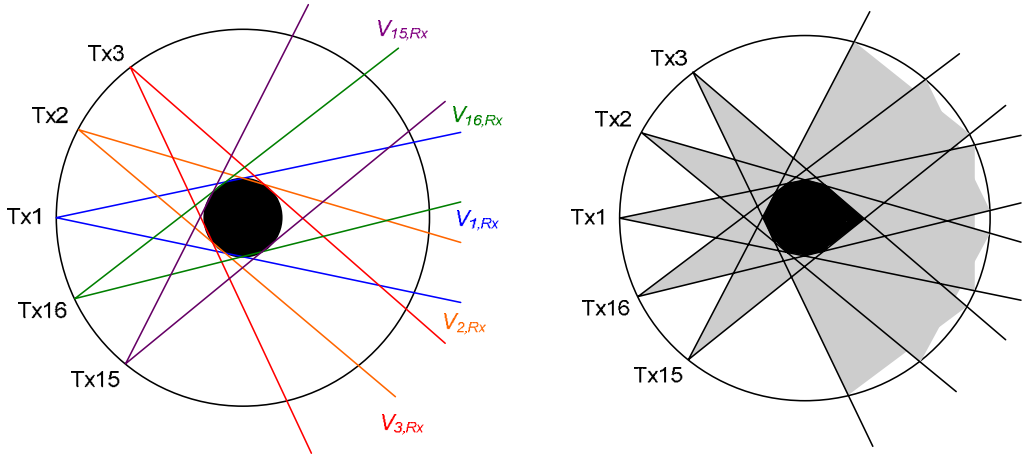

a) Projection

b) Back Projection

Figure 2 The fan-shaped beam back projection

The density of each point in the reconstructed image is obtained by summing up the densities of all rays which pass through that point. This process may be described by Equation 1. Equation 1 is the back projection algorithm where the spoke pattern represents blurring of the object in space.

$$f_b(x,y) = \sum_{j=1}^{m} g_j(x\cos\theta_j + y\sin\theta_j)\Delta\theta \qquad (1)$$

where $f_b(x, y)$ = the function of reconstructed image from back projection algorithm, θ_j = the j-th projection angle and $\Delta\theta$ = the angular distance between projection and the summation extends over all the m projection

Ultrasonic flow imaging systems require quite different reconstruction algorithms because of the form in which the measured data is obtained. Essentially, it is due to a set of time delay measurements that gives the distance of object media interfaces from the receiving sensors [3]. Besides, the ultrasound propagation depends on the medium; which in this case focuses on liquid/gas medium. The uncertain liquid condition such as wavy may also lead to the uncertain sensor values and as well as the reconstructed images.

2.0 LINEAR BACK PROJECTION ALGORITHM

In Linear Back Projection (LBP) algorithm, the concentration profile is generated by combining the projection data from each sensor with its computed sensitivity maps [4]. The modelled sensitivity matrices are used to represent the image plane for each view. To reconstruct the image, each sensitivity matrix is multiplied by its corresponding sensor loss value; this is same as back projecting each sensor loss value to the image plane individually [2]. Then, the same elements in these matrices are summed to provide the back projected voltage distributions (concentration profile) and finally these voltage distributions will be represented by the colour level (coloured pixels). This process can be expressed mathematically as below [2]:

$$V_{LBP}(x, y) = \sum_{Tx=1}^{m} \sum_{Rx=1}^{n} S_{Tx,\,Rx} \times \overline{M}_{Tx,\,Rx}(x, y) \tag{2}$$

where $V_{LBP}(x, y)$ = voltage distribution obtained using LBP algorithm in the concentration profile matrix and $S_{Tx,Rx}$ = sensor loss voltage for the corresponding transmission (Tx) and reception (Rx).

3.0 HYBRID RECONSTRUCTION ALGORITHM

The Hybrid Reconstruction (HR) algorithm is based on the previous development by Ibrahim [5]. This algorithm determines the condition of projection data and improves the reconstruction by marking the empty area during image reconstruction. As a result, the smearing effect caused by the back projection technique is reduced. The projection data obtained by Ibrahim [5] is based on the sensor value. Later, Chan [6] used a different approach where he used the signal

loss measurement instead of direct projection data in order to reconstruct the fan-shaped beam image through optical technique. He claimed that this method is easier to implement compared to the original method. The HR is obtained by multiplying the concentration profile obtained using the LBP with the HR masking matrix.

The HR masking matrix was obtained by filtering each of the concentration profile element. If the concentration profile element is larger or equal to ¾ of the maximum pixel value, then the masking matrix element for the corresponding concentration profile element is set to one otherwise it is set to zero. The mathematical model for HR is shown as below:

$$V_{HR}(x, y) = B_{HR}(x, y) \times V_{LBP}(x, y) \tag{3}$$

in which:

$$\begin{aligned} B_{HR}(x, y) = 0 &\Rightarrow V_{LBP}(x, y) < P_{Th} \\ B_{HR}(x, y) = 1 &\Rightarrow V_{LBP}(x, y) \geq P_{Th} \end{aligned} \tag{4}$$

where B_{HR} (x, y) = HR masking matrix, P_{Th} = pixel threshold value (¾ of the maximum value), $V_{LBP}(x, y)$ = reconstructed concentration profile using LBP and $V_{HR}(x, y)$ = improved concentration profile using HR.

4.0 HYBRID BINARY RECONSTRUCTION ALGORITHM

For comparison with the LBP and HR method, another image reconstruction technique has been employed namely the Hybrid Binary Reconstruction (HBR) algorithm. This algorithm has the advantage of improving the stability and repeatability of the reconstructed image. The HBR is obtained by multiplying each sensor value to its corresponding sensitivity map. If the sensor value is higher or equal to the threshold voltage, (V_{Th}) then its projection path which is represented by the sensitivity map is set to a maximum pixel value (i.e 511), otherwise it is set to a minimum pixel value (i.e. 0).

If the projection path consist of discontinuous component (gas), the transmitted ultrasound energy will be totally reflected and thus no ultrasound signal detected at the receiver. Therefore, a threshold voltage must be first selected. This threshold voltage is needed for the purpose of separating the object from the background, thus creating a binary picture from a picture data (tomogram). This procedure is only appropriate for two-phase flow imaging in cases where the phases are well separated such as liquid-gas flow [7].

Besides, the dynamic characteristic of liquid-gas flow is most probably uncertain and it is quite hard to predict the behaviour of such flow. For industrial

flow, the sudden changes in term of pressure lead to wavy flow. This may result the sensor value to fluctuate randomly and causes to the unknown image reconstructed as well as increases the measurement error. By thresholding the sensor value, it limits the sensor value fluctuation and therefore minimizes the measurement error. The mathematical model for HBR is shown as follows:

$$V_{HBR}(x, y) = \sum_{Tx=1}^{m} \sum_{Rx=1}^{n} V_{Tx,\,Rx} \times \overline{M}_{Tx,\,Rx}(x, y) \tag{5}$$

in which

$$\begin{aligned} V_{HBR}(x, y) = 0 \quad &\Rightarrow V_{Tx,\,Rx} < V_{Th} \\ V_{HBR}(x, y) = 511 \quad &\Rightarrow V_{Tx,\,Rx} \geq V_{Th} \end{aligned} \tag{6}$$

where $V_{Tx,Rx}$ = the sensor value and $V_{HBR}(x, y)$ = concentration profile obtained using HBR

The reconstruction method is represented in the flow chart in Figure 3.

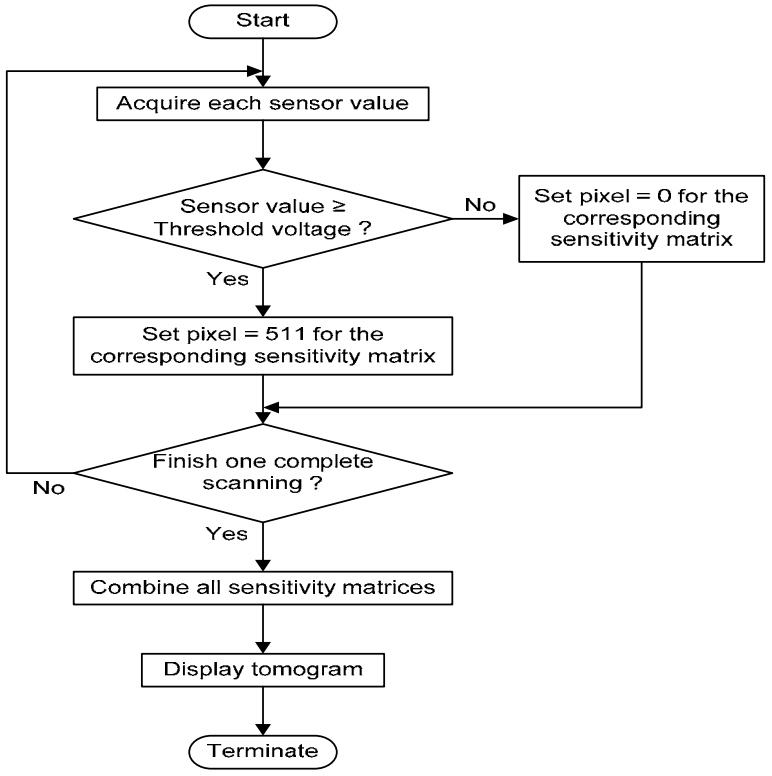

Figure 3 The HBR flowchart

5.0 IMAGE RECONSTRUCTION ERROR MEASUREMENT

The quality of a tomographic flow imaging system can be judged by comparing the reconstructed image of a physical model with the actual cross-section [8]. The comparison is performed on the image reconstruction computer against a standard image (test model) which matches the cross-section of the physical model. The image plane representing the cross-section of the experimental column is divided into M square image pixels. A 64 × 64 array pixels image has been chosen for displaying the reconstructed image. Thus, M = 3320 pixels where another 776 pixels lie outside the column boundary. Ideally, the reconstructed image should be identical to the standard image (the test model), but in practice differences arise. To quantify these differences, error information is obtained using the area error, AE, which is defined as below [9]:

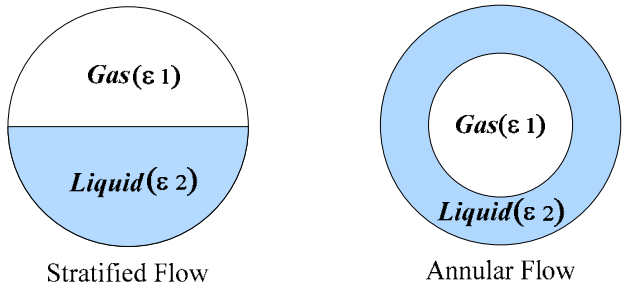

Figure 4 Image reconstruction error measurement models

The standard image in Figure 4 is an array of M pixels defining the standard (test) model by the colour level of each pixel:

$$G_S(p) = \begin{cases} 0 & \text{for pixels occupied by Gas component } (\varepsilon_1) \\ G_M & \text{for pixels occupied by Liquid component } (\varepsilon_2) \end{cases} \tag{7}$$

$$G_B(p) = \begin{cases} 0 & G_R(p) = 0 \\ G_M & G_R(p) > 0 \end{cases} \qquad (p = 1,2,...,M) \tag{8}$$

in which:

$$AE = \frac{\sum_{p=1}^{M} G_B(p) - \sum_{p=1}^{M} G_S(p)}{\sum_{p=1}^{M} G_S(p)} = \frac{N_R - N_S}{N_S} = \frac{N_R}{N_S} - 1 \tag{9}$$

where $G_S(p)$ = the standard (test) model pixels, $G_M(p)$ = the colour level assigned to the liquid component, $G_B(p)$ = the binary reconstructed image pixels, N_R = the number of pixels with non-zero colour levels in the reconstructed images and N_S = the number of pixels with non-zero colour levels in the standard images.

However, *AE* value is preferably presented in percentages by multiplying with 100%. The value of *AE* that negative indicates that the reconstructed object is always smaller than the standard models whereas the positive value of *AE* indicates the reconstructed object is always larger compared to the standard models.

6.0 RESULTS

In this section, results for the reconstruction algorithm simulations of several test profiles and the real-time reconstructed images for several experiments are presented and discussed. The experiments involve simulation from the forward models and real-time measurement on the test profiles for stratified and annular flows.

6.1 The Stratified Flows

Stratified flow regime is created by placing the experimental column horizontally such that the gas phase (air) flows in the upper section of the column and the liquid (water) in the lower section. A horizontal column with static liquid model was used to simulate the stratified flow.

The liquid component was determined from 10% flow to 100% flow with an increment of 5% for each measurement taken and it has been used as the standard model. The *Area Error* (*AE*) has been calculated for the real-time measurement made using LBP, HR and HBR in the stratified flows based on Equation 9 and it is shown in Figure 5. The tomogram images for three quarter flow of forward model and real-time measurement are shown in Figure 6.

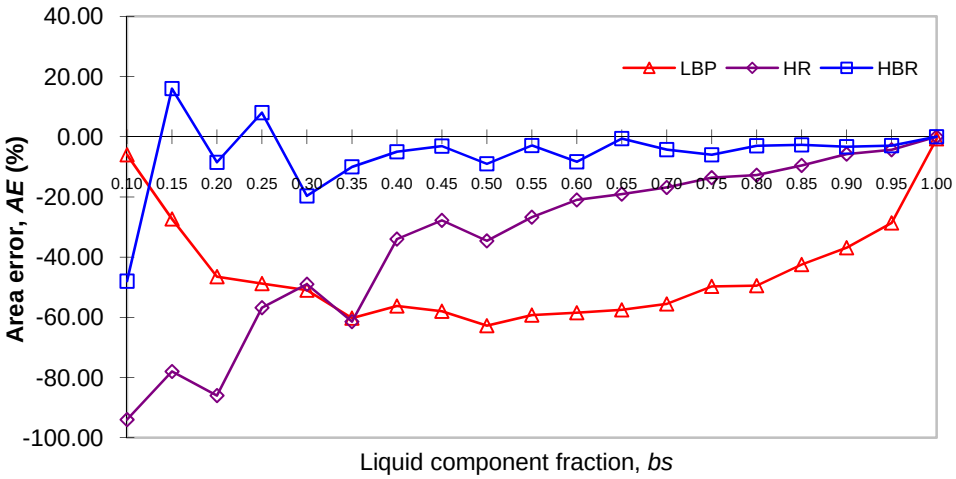

Figure 5 *AE* for the stratified flow

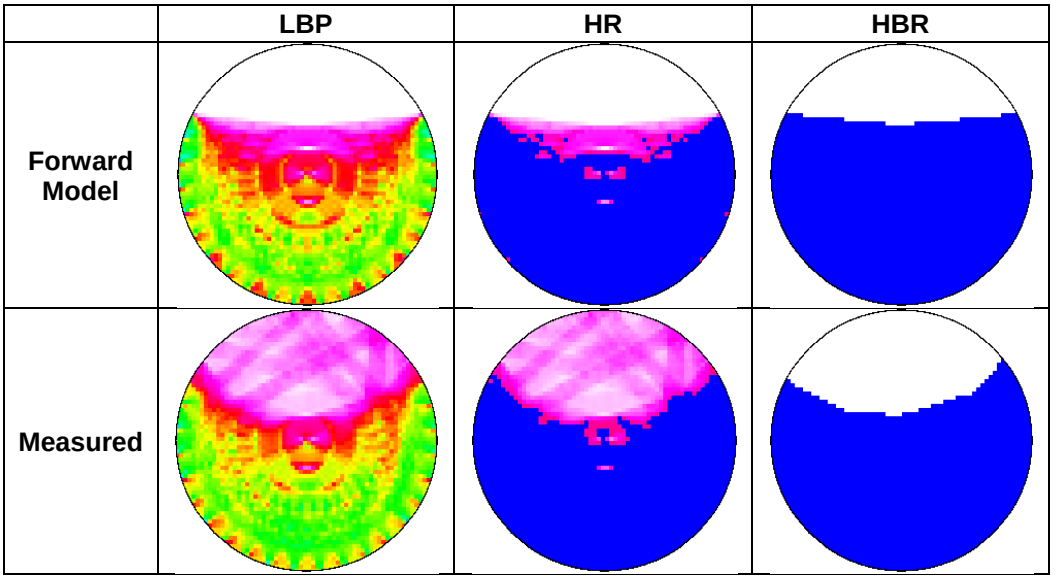

Figure 6 The tomograms for three quarter flow of forward model and real-time measurement

In stratified flow, the reconstructed images by LBP produced a lot of smearing effects. Meanwhile, the *Area Error* (*AE*) was found highest during the half flow that is -62.8% and the lowest value during full liquid flow that is -0.7%. On the other hand, the reconstructed images by HR are more likely affected by these smearing effects. As shown in Figure 6, the smearing effects are mostly contributed

by high pixel values. Thus, the threshold in the HR seems unable to reduce this false image.

Compared to LBP and HR, the HBR had removed these false images completely. The image reconstructed by HBR mostly preserved their shapes and positions and therefore the stratified flow regime can be clearly identified. However, the HBR is not superior during low liquid flow especially at α = 0.1 which has *Area Error* of -48%. It is because during low liquid flow, most of the column section is occupied by the gas component which provide high acoustic impedance region. Thus, the number of measurement has been limited to low acoustic impedance in the liquid segment. The *Area Error* in HBR reconstruction however tends to improve as the liquid component fraction increases.

6.2 The Annular Flows

Annular flow regime is obtained when an empty circular tube (gas model) was inserted in the centre of the column and the gap between the tube and column was filled with liquid (water). Several test models with different diameters were used to simulate multi-diameter annular flow regime. The annular flow model diameter, A_d are 21.6 mm, 27.0 mm, 33.7 mm, 42.2 mm, 48.6 mm, 60.5 mm and 82.8 mm. Using the same approach, the *Area Error* for annular flow is calculated and shown in Figure 7. The tomogram images for annular flow of forward model and real-time measurement are shown in Figure 8.

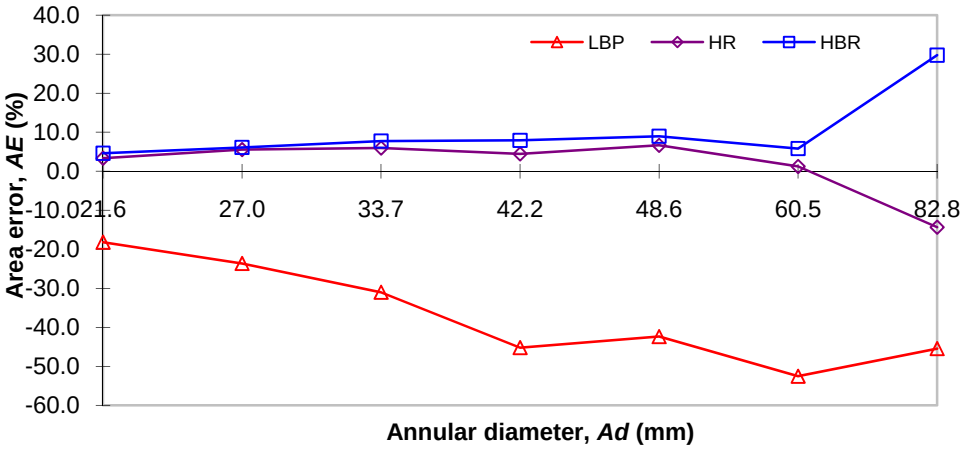

Figure 7 *AE* for the annular flow

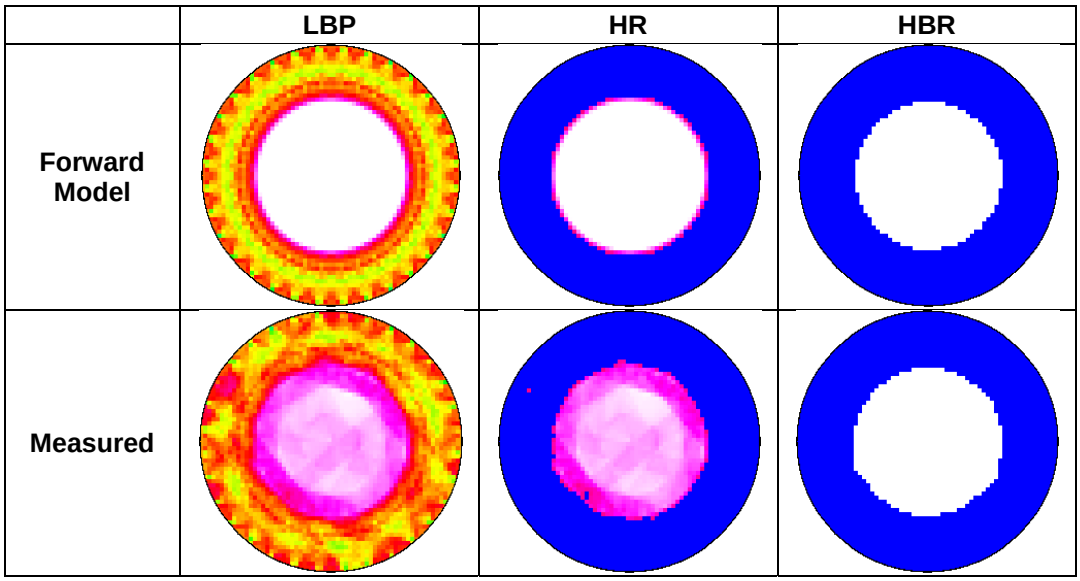

Figure 8 The tomograms for annular flow of forward model and real-time measurement

In annular flow, the reconstructed images by LBP and HR have not been much affected by the smearing effects of back projection technique. In this case, the reconstructed image clearly indicates the annular flow segment. In addition, the shape and position of annular flow which consist of liquid/gas component is more or less the same with the simulated flow regime. From Figure 7, it is found that the *Area Error* increases as the annular flow diameter increases. This is because the false image which filled the gas section contributes to the error statistics.

From the observations, it is found that the *Area Error* by HR and HBR techniques are almost constant. For HBR, it showed that the reconstructed images are always larger than the test model. This phenomena is because, HBR reconstruct image using the sensor value. Thus, the reconstructed image depends on the sensor's resolution and also the number of measurements taken.

7.0 CONCLUSIONS

This paper presents three types of image reconstruction algorithm namely the Linear Back Projection (LBP), Hybrid Reconstruction (HR) and Hybrid Binary Reconstruction (HBR). Two types of flow regimes namely three quarter and annular flow had been tested using these algorithms. Measurements showed that, the image reconstructed by LBP results in blurring image which leads to high *AE*

in every measurement taken. This blurring image is due to the nature of back projection technique. However, the blurring image is reduced by using HR algorithm but smearing effects of high pixel value is still obvious. Implementing the HBR algorithm had eliminated all the smearing effects and resulted in the lowest *Area Errors* in overall reconstructions. Thus, the HBR has become the most suitable reconstruction algorithm for liquid and gas flow compared to LBP and HR algorithms.

REFERENCES

[1] Garcia-Stewart, C. A., Polydorides, N., Ozanyan, K. B. and McCann, H. Image Reconstruction Algorithms for High-Speed Chemical Species Tomography. *2003*. Proceedings 3rd World Congress on Industrial Process Tomography. Banff, Canada. 80-85.

[2] M. H. F. Rahiman, R. A. Rahim, M. H. F. Rahiman, and M. Tajjudin. 2006. Ultrasonic Transmission-Mode Tomography Imaging for Liquid/Gas Two-Phase Flow. *IEEE Sensors J*. 6(6): 1706–1715.

[3] R. Abdul Rahim, M. H. Fazalul Rahiman, K.S. Chan, S.W. Nawawi. 2007. Non-Invasive Imaging Of Liquid/Gas Flow Using Ultrasonic Transmission-Mode Tomography. *Sensors And Actuators A*. 135: 337–345.

[4] McKeen, T. R. and Pugsley, T. S. 2002. The Influence of Permittivity Models on Phantom Images Obtained From Electrical Capacitance Tomography. *Measurement Science Technology*. 13: 1822-1830.

[5] Ibrahim, S. 2000. *Measurement of Gas Bubbles in A Vertical Water Column Using Optical Tomography*. Sheffield Hallam University: Ph.D. Thesis.

[6] Chan, K. S. 2002. *Real Time Image Reconstruction for Fan Beam Optical Tomography System*. Universiti Teknologi Malaysia: M.Eng. Thesis.

[7] Plaskowski, A., Beck, M. S., Thron, R., Dyakowski, T. 1995. *Imaging Industrial Flows: Applications of Electrical Process Tomography*. U.K.: IOP Publishing Ltd.

[8] Aleman, C. O., Martin, R. and Gamio, J. C. 2004. Reconstruction of Permittivity Images From Capacitance Tomography Data by Using Very Fast Simulated Annealing. *Measurement Science Technology*. 15: 1382-1390.

[9] Xie, C. G., Huang, S. M., Lenn, C. P., Stott, A. L., Beck, M.S. 1994. Experimental Evaluation of Capacitance Tomographic Flow Imaging Systems Using Physical Models. *IEE Proc. Circuits Devices System*. 141(5): 357-368.